



# HHS Public Access

Author manuscript

*Mol Pharm.* Author manuscript; available in PMC 2020 August 05.

Published in final edited form as:

*Mol Pharm.* 2019 August 05; 16(8): 3534–3543. doi:10.1021/acs.molpharmaceut.9b00369.

## Plasma pharmacokinetics of high-affinity transferrin receptor antibody-erythropoietin fusion protein is a function of effector attenuation in mice

Jiahong Sun<sup>1</sup>, Ruben J. Boado<sup>2</sup>, William M. Pardridge<sup>2</sup>, Rachita K. Sumbria<sup>1,3</sup>

<sup>1</sup>Department of Biopharmaceutical Sciences, School of Pharmacy and Health Sciences, Keck Graduate Institute, Claremont, CA 91711

<sup>2</sup>ArmaGen, Inc., Agoura Hills, CA 91301

<sup>3</sup>Departments of Neurology, University of California, Irvine, CA 92868

### Abstract

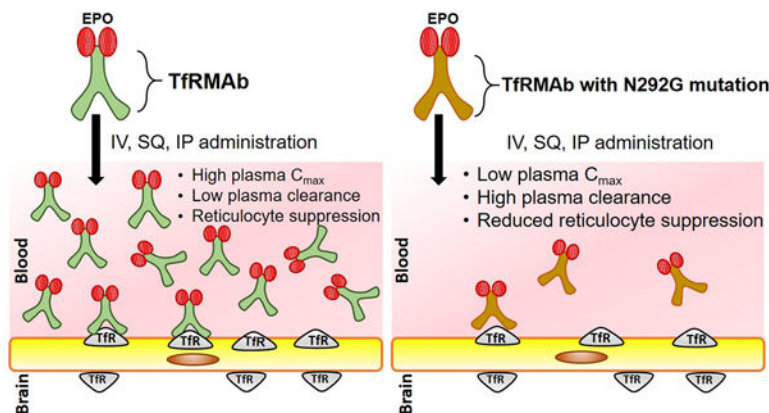
Erythropoietin (EPO) is a potential therapeutic for Alzheimer's disease (AD), however limited blood-brain barrier (BBB) penetration reduces its applicability as a CNS therapeutic. Antibodies against the BBB transferrin receptor (TfRMABs) act as molecular Trojan horses for brain drug delivery, and a fusion protein of erythropoietin (EPO) and TfRMAB, designated TfRMAB-EPO, is protective in a mouse model of AD. TfRMABs have Fc effector function side-effects, and removal of the Fc N-linked glycosylation site by substituting Asn with Gly reduces Fc effector function. However, the effect of such Fc mutations on the pharmacokinetics of plasma clearance of TfRMAB-based fusion proteins, such as TfRMAB-EPO, is unknown. To examine this, the plasma pharmacokinetics of TfRMAB-EPO (wild-type), which expresses the mouse IgG1 constant heavy chain region and includes the Asn residue at position 292, was compared to the mutant TfRMAB-N292G-EPO, in which the Asn residue at position 292 is mutated to Gly. Plasma pharmacokinetics were compared following IV, IP and SQ administration for doses between 0.3–3 mg/kg in adult male C57 mice. The results show a profound increase in clearance (6- to 8-fold) of the TfRMAB-N292G-EPO compared with the wild-type TfRMAB-EPO following IV administration. The clearance of both the wild-type and mutant TfRMAB-EPO fusion proteins followed non-linear pharmacokinetics, and a 10-fold increase in dose resulted in a 7- to 11-fold decrease in plasma clearance. Following IP and SQ administration, the  $C_{max}$  values of the TfRMAB-N292G-EPO mutant were profoundly (37- to 114-fold) reduced compared with the wild-type TfRMAB-EPO, owing to comparable increases in plasma clearance of the mutant fusion protein. The wild-type TfRMAB fusion protein was associated with reticulocyte suppression, and the N292G mutation mitigated this suppression of reticulocytes. Overall, the beneficial suppression of effector function via the N292G mutation may be offset by the deleterious effect this mutation has on the plasma levels of the TfRMAB-EPO fusion protein, especially following SQ administration, which is the preferred route of administration in humans for chronic neurodegenerative diseases including AD.

**Address correspondence to:** Rachita K. Sumbria, PhD, Department of Biopharmaceutical Sciences, School of Pharmacy and Health Sciences, Keck Graduate Institute, Claremont, CA, 91711, Tel: (909) 607-0319, Fax: (909) 607-9826, rsumbria@kgi.edu.

Conflict of Interest

William Pardridge is a consultant to and Ruben Boado is an employee of ArmaGen, Inc.

## Graphical Abstract



## Keywords

transferrin receptor; blood-brain barrier; molecular Trojan horses; Fc effector function side-effects; pharmacokinetics

## Introduction

Neurological disorders are a leading cause of disability worldwide with limited treatment options. A growing class of drugs under development for neurological disorders is biologic drugs including recombinant proteins, therapeutic antibodies, decoy receptors, neurotrophins, enzymes, peptides and nucleic acid therapies.<sup>1</sup> One major obstacle to the development of such biologic therapies for the brain is the blood-brain barrier (BBB).<sup>2</sup> Among the drug delivery strategies to overcome the BBB, targeting of endogenous receptor-mediated transcytosis (RMT) systems was introduced more than 30 years ago and continues to be a promising approach to ferry biologics into the brain across an intact BBB.<sup>3</sup> The transferrin receptor (TfR) is one such RMT system that is expressed at the BBB, and antibodies directed against the TfR (TfrMAb) have received significant attention in the last decade as brain drug delivery vectors.<sup>3–6</sup>

The original work with the TfrMAbs as molecular Trojan horses (MTHs) for brain drug delivery involved the high-affinity rat/mouse IgG1 chimeric bivalent TfrMAb.<sup>3, 7</sup> This high-affinity TfrMAb readily binds the mouse TfR with a  $K_D = 2.6 \pm 0.3$  nM, and fusion proteins of this TfrMAb and biologic drugs, including decoy receptors,<sup>8</sup> neurotrophins,<sup>9</sup> and therapeutic antibodies,<sup>10</sup> have been engineered and tested in mouse models of neural disease. Typical injection dose (ID) for a high-affinity TfrMAb in the mouse is 1 mg/kg by intravenous (IV) administration.<sup>3</sup> TfrMAbs have also been engineered with low-affinity TfR binding ( $K_D = 111 \pm 1.6$  nM).<sup>5</sup> The ID of a low-affinity TfrMAb is 20–50 mg/kg IV,<sup>4</sup> which is 20–50 fold higher than the IV ID of a high-affinity TfrMAb that produces therapeutic effects in experimental models of neural disease.<sup>11–12</sup>

A single injection of a TfrMAb in the mouse induces effector function side-effects, which include injection related reactions (IRR) and suppressed reticulocyte counts in blood.<sup>4, 6, 13</sup>

The mutation of a single Fc region asparagine (Asn) residue, which is the site of IgG glycosylation, eliminates binding of the IgG to the Fc gamma receptor (Fc $\gamma$ R), but has no effect on IgG binding to the neonatal Fc receptor (FcRn).<sup>14–15</sup> The N297G mutation eliminates the suppression of blood reticulocytes caused by administration of a TfRMAB in the primate,<sup>13</sup> and partially resolves this effect on blood reticulocytes in the mouse.<sup>4, 16</sup> The N297G mutation causes no change in the pharmacokinetics (PK) of plasma clearance of a monoclonal antibody, not directed against the TfR, in either the primate<sup>17</sup> or mouse.<sup>18</sup> The N297G mutation also has no effect on the plasma clearance of a low-affinity TfRMAB following the IV administration of an ID dose of 50 mg/kg in the mouse.<sup>16</sup> The high ID, 50 mg/kg, of a low-affinity TfRMAB may saturate systemic clearance mechanisms that have a high affinity for the TfRMAB, and the extent to which the Asn mutation alters the PK of plasma clearance of a high-affinity TfRMAB that is administered at a lower dose of 1–3 mg/kg IV is not known.

Erythropoietin (EPO), a 30.4 kDa glycoprotein, is protective in rodent models of Alzheimer's disease (AD), however, has limited BBB penetration.<sup>19–20</sup> Our recent work shows that EPO fused to a high-affinity TfRMAB offers therapeutic benefits in the APP/PS1 double transgenic mouse model of AD.<sup>9</sup> This TfRMAB-EPO fusion protein expresses the mouse IgG1 constant heavy chain (HC) region, which includes the Asn residue at position 292. The present investigation measures the PK of plasma clearance of this high-affinity TfRMAB-EPO fusion protein with and without the Fc Asn to Gly (N292G) mutation. The PK of plasma clearance of the non-mutated wild-type (WT) TfRMAB-EPO fusion protein and the TfRMAB-N292G-EPO fusion protein is examined after the IV administration of 0.3 and 3 mg/kg doses. Given that long-term treatment of AD will require more frequent administration, the effect of the N292G mutation on the plasma clearance of the fusion protein is also examined in these investigations after subcutaneous (SQ) and intraperitoneal (IP) administration of the TfRMAB-EPO fusion proteins.

## Experimental Section

### TfRMAB-EPO fusion proteins

The TfRMAB-EPO fusion protein was produced in stably transfected Chinese hamster ovary (CHO) cells and purified by Protein G affinity chromatography, and formulated at a concentration of 0.7 mg/mL in 98 mM glycine, 148 mM NaCl, 28 mM Tris, 0.01% Polysorbate 80, pH=5.5, sterile filtered and stored at –80°C till use, as described previously.<sup>21</sup> The TfRMAB-N292G-EPO fusion protein with a single N292G mutation in the HC was produced by Genscript (Piscataway, NJ) in ExpiCHO cells that were grown in serum-free ExpiCHO Expression Medium (Gibco, Gaithersburg, MD). The TfRMAB-N292G-EPO fusion protein was affinity purified with a Protein G column and the Protein G eluate was further purified by Superdex 200 preparative grade size exclusion chromatography (SEC). The purified TfRMAB-N292G-EPO fusion protein was analyzed using reducing and non-reducing SDS-PAGE, SEC HPLC, and endotoxin for the assessment of protein molecular weight and purity. The mutant fusion protein was formulated at a concentration of 0.78 mg/mL in 98 mM glycine, 148 mM NaCl, 28 mM Tris, 0.01% Polysorbate 80, pH=5.5, sterile filtered and stored at –80°C till use.

## Plasma pharmacokinetics in the mouse

All animal procedures were approved by the University of La Verne Institutional Animal Care and Use Committee. Eight-week old male C57BL/6J mice weighing 25–27 g were obtained from the Jackson Laboratory (Bar Harbor, ME). Mice were provided constant access to food and water and maintained on a 12 h light/12 h dark cycle. Mice were randomly assigned to treatment groups and the TfRMAb-EPO and TfRMAb-N292G-EPO fusion proteins were injected in different experiments via IV, IP, or SQ routes in the volume of 80–120  $\mu\text{L}$  per mouse. Mice received a single injection of the fusion protein at the dose of 0.3 mg/kg or 3 mg/kg for IV PK, or 3 mg/kg for IP and SQ PK. Each treatment group comprised of 3–6 mice for each injection dose. An aliquot of blood in sodium citrate (9 parts blood and 1 part sodium citrate) was collected via the retro-orbital sinus at 2, 5, 15 and 60 min after IV-, at 1, 3, 6 and 24 h following IP- and at 3, 6 and 24 h following SQ-administration. After collection, blood samples were centrifuged at 12,000 rpm at 4°C for 5 min and plasma was collected to determine the concentration of the fusion proteins.

## Measurement of reticulocytes

Twenty-four hours after IV, IP or SQ injections, 140  $\mu\text{L}$  aliquot of blood was collected via the retro-orbital sinus and shipped overnight at 4°C to Molecular Diagnostic Services, Inc. (San Diego, CA) for the measurement of reticulocyte counts.

## TfR binding assay

Binding of the WT and mutant TfRMAb-EPO fusion proteins to TfR was confirmed by the TfR ELISA. Briefly, Nunc Maxisorp 96 well ELISA plates (Fisher Scientific, Waltham, MA) were coated with mouse TfR (R&D system, Minneapolis, MN) overnight at 4°C (200 ng/well) and blocked with tris-buffered saline (TBS) containing 1% bovine serum albumin (TBSB) for 1h at room temperature. Increasing concentrations (0.3–9000 ng/well) of TfRMAb-EPO and TfRMAb-N292G-EPO fusion proteins were added to the wells (100  $\mu\text{L}$ /well) and incubated for 1h followed by washing with TBS containing 0.05% Tween-20 (TBST). Wells were incubated with 400 ng/well of rabbit anti-EPO antibody (R&D system, Minneapolis, MN) in TBSB for 30 min at room temperature, followed by 3 washes with TBST. Wells were then incubated with 500 ng/well of goat anti-rabbit IgG –H+L (GAR) secondary antibody-alkaline phosphatase (AP) conjugate (GAR-AP) (Vector Laboratories, Burlingame, CA) for 45 min at room temperature. After washing with TBST, wells were incubated with P-nitrophenyl phosphate (Sigma-Aldrich, St. Louis, MO) for 30 min in the dark, and the reaction was stopped by adding 100  $\mu\text{L}$  of 1.2M NaOH per well. Absorbance (OD) was measured at 405 nm and standard curves were fit to the two site-specific binding nonlinear regression curve to determine maximal binding ( $B_{\text{max}}$ ) and dissociation constant ( $K_d$ ) values using GraphPad Prism 8 (San Diego, CA). TBSB blank corrected OD values were used.

## EPO receptor (EPOR) binding assay

The binding to EPOR and the concentration of the TfRMAb-EPO and TfRMAb-N292G-EPO fusion proteins in mouse plasma were determined by an EPOR ELISA. Briefly, 100  $\mu\text{L}$  per well of 2  $\mu\text{g}/\text{mL}$  of the EPOR/Fc fusion protein (R&D system, Minneapolis, MN) was

used to pre-coat Nunc Maxisorp 96 well ELISA plates (Fisher Scientific, Waltham, MA) at 4°C overnight. The wells were washed with TBST followed by blocking with TBSB for 1h at room temperature. Plasma samples or standards (0.3–9000 ng/well of TfRMAb-EPO and TfRMAb-N292G-EPO fusion proteins) were added to the wells (100 µL/well) and incubated for 2h followed by washing with TBST. Wells were then incubated with 100 ng/well of goat anti-mouse light chain (kappa) antibody conjugated to alkaline phosphatase (Bethyl Laboratories, Inc., Montgomery, TX) for 45 min at room temperature. After washing with TBST, wells were incubated with P-nitrophenyl phosphate (Sigma-Aldrich, St. Louis, MO) for 30 min in the dark, and the reaction was stopped by adding 100 µL of 1.2M NaOH per well. OD was measured at 405 nm and standard curves were fit to the one site-specific binding nonlinear regression curve to determine  $B_{max}$  and  $K_d$  values using GraphPad Prism 8 (San Diego, CA). The plasma concentrations of fusion protein were calculated as follows:  $Concentration = (OD \times K_d) / (B_{max} - OD)$ . TBSB blank corrected OD values were used. Plasma concentration data were expressed as (a) plasma concentration (µg of fusion protein per mL plasma) and (b) percent of ID/mL. To exclude any influence of the plasma matrix on the assay results, a parallelism test was performed to validate the ELISA assay for which TBSB (blank) and mouse plasma were spiked with 900 ng/mL of TfRMAb fusion protein. ELISA assay results showed similar OD values between TBSB and mouse plasma samples for dilutions up to 1:640, indicating good parallelism between the OD measurements.

### Pharmacokinetic analysis

Non-compartmental analysis was performed on the plasma concentration-time data using Thermo Scientific Kinetica 5.0 (ThermoFisher Scientific, Waltham, MA) to calculate PK parameters for the TfRMAb-EPO and TfRMAb-N292G-EPO fusion proteins. The parameters calculated included the maximum plasma concentration ( $C_{max}$ ), mean residence time (MRT), area under the plasma concentration-time curve (AUC), volume of distribution at steady-state ( $V_{ss}$ ), clearance and bioavailability. The  $AUC(0-\infty)$  following IV administration was used as an approximation to  $AUC(0-24h)$  for bioavailability estimation.

### Cell Proliferation

Murine brain microvascular endothelial cells (bEND3 cells; American Type Culture Collection, Manassas, VA) between passages 22 and 31 were grown on T75 flasks in Delbucco's Modified Eagle's Medium (DMEM) with 10% fetal bovine serum, and 100µg/ml penicillin/streptomycin (Sigma, St. Louis, MO). After reaching 70–80% confluency, cells were seeded onto 96-well plates ( $3 \times 10^3$  bEND3 cells per well), and treated with either recombinant human EPO (rhuEPO; 10 ng/mL since EPO is 20% of the TfRMAb-EPO based on molecular weight), TfRMAb-EPO (50 ng/mL) or TfRMAb-N292G-EPO (50 ng/mL) all formulated in 98 mM glycine, 148 mM NaCl, 28 mM Tris, 0.01% Polysorbate 80, pH=5.5. Untreated bEND3 and vehicle treated bEND3 served as controls. After 4 days, media was removed, wells were washed with ice cold PBS three times followed by incubation with 100µL of DMEM with 10µL of cell-counting kit-8 (CCK-8) reagent at 37°C for 3 h as per manufacturer's instructions (Dojindo Molecular Technologies, Inc., Rockville, MD). OD was measured at 450 nm, and media-only blank corrected OD values were reported as percentage of OD values of the bEND3 group.



## Statistical analysis

Data are represented as mean  $\pm$  SEM and all statistical analysis was performed using GraphPad Prism 8 (GraphPad Software Inc., La Jolla, CA). Two-way ANOVA with Bonferroni's post hoc test and one-way ANOVA with Holm-Sidak's multiple comparisons test were used to compare reticulocyte counts and cell proliferation, respectively. A two-tailed p-value of  $<0.05$  was considered statistically significant.

## Results

### Protein Characteristics

The ExpiCHO-derived TfRMAb-N292-EPO was detected with the estimated molecular weights of ~25 kDa and ~68 kDa respectively under reducing conditions (lane 2), and ~200 kDa under non-reducing conditions (lane 3) by SDS-PAGE analysis (Figure 1A). Both the WT and mutant TfRMAb-EPO retained comparable high-affinity binding to both the TfR (Kd: TfRMAb-EPO =  $15.8 \pm 4.1$  ng/mL, TfRMAb-N292G-EPO =  $9.9 \pm 2.1$  ng/mL) and EPOR (Kd: TfRMAb-EPO =  $15.2 \pm 1.9$  ng/mL, TfRMAb-N292G-EPO =  $10.3 \pm 0.61$  ng/mL) as shown in figures 1B and C. Conversely, equivalent concentrations based on amino acid (AA) sequence of rhuEPO did not show any binding to the TfR (Figure 1B).

### Plasma pharmacokinetics after IV administration

Plasma concentrations-time curves following a single 3 mg/kg IV dose of the TfRMAb-EPO or TfRMAb-N292G-EPO are shown in Figure 2, and are expressed as either  $\mu\text{g/mL}$  (Figure 2A) or  $\%ID/mL$  (Figure 2B). Using non-compartmental analysis, the  $C_{\text{max}}$  following IV administration of a single IV 3 mg/kg dose was  $21.6 \pm 2.7$   $\mu\text{g/mL}$  for the WT TfRMAb-EPO fusion protein. The  $C_{\text{max}}$  of the TfRMAb-N292G-EPO fusion protein was  $13.5 \pm 1.1$   $\mu\text{g/mL}$ , which is 2-fold lower than that of the WT TfRMAb-EPO fusion protein (Table 1). At 1h following IV administration, the plasma concentration of TfRMAb-EPO decreased to  $9.7 \pm 1.7$   $\mu\text{g/mL}$  ( $13 \pm 2.4$   $\%ID/mL$ ), while the plasma concentration was 36-fold lower at  $0.27 \pm 0.65$   $\mu\text{g/mL}$  ( $0.37 \pm 0.087$   $\%ID/mL$ ) for the TfRMAb-N292G-EPO fusion protein (Figure 2). The plasma AUC (Table 1) of the WT fusion protein ( $2,045 \pm 868$   $\mu\text{g}\cdot\text{min/mL}$ ) was 9-fold higher than that of the N292G mutant fusion protein ( $219 \pm 70$   $\mu\text{g}\cdot\text{min/mL}$ ), consistent with low plasma concentrations of TfRMAb-N292G-EPO. The plasma clearance of the TfRMAb-N292G-EPO fusion protein ( $14.9 \pm 4.7$  mL/min/kg) was 8-fold faster, while the MRT ( $11.6 \pm 2.9$  min) was 10-fold shorter compared with the clearance and MRT of the TfRMAb-EPO fusion protein (clearance:  $1.8 \pm 0.9$  mL/min/kg; MRT:  $116 \pm 64$  min) (Table 1).

Plasma concentrations-time curves following a single 0.3 mg/kg IV dose of the TfRMAb-EPO and TfRMAb-N292G-EPO fusion proteins are shown in Figure 3. Using non-compartmental analysis, the  $C_{\text{max}}$  value was  $0.94 \pm 0.3$   $\mu\text{g/mL}$  for the TfRMAb-EPO fusion protein and declined 3-fold to  $0.31 \pm 0.09$   $\mu\text{g/mL}$  for the mutant TfRMAb-EPO fusion protein (Table 1). At 1h following a single injection of a 0.3 mg/kg IV dose, the plasma concentrations of the WT and mutant TfRMAb fusion proteins were  $0.067 \pm 0.01$   $\mu\text{g/mL}$  ( $1.0 \pm 0.2$   $\%ID/mL$ ) and  $0.010 \pm 0.002$   $\mu\text{g/mL}$  ( $0.14 \pm 0.002$   $\%ID/mL$ ), respectively, which is a 7-fold decline in the plasma concentration for the mutant fusion protein (Figures 3A–B). The plasma AUC of the WT fusion protein ( $16.9 \pm 6.1$   $\mu\text{g}\cdot\text{min/mL}$ ) was 6-fold higher than

that of the N292G mutant fusion protein ( $2.9 \pm 1.1 \mu\text{g} \cdot \text{min}/\text{mL}$ ), consistent with the lower plasma concentrations of the mutant fusion protein. The plasma clearance of the TfRMAB-N292G-EPO fusion protein ( $110 \pm 34 \text{ mL}/\text{min}/\text{kg}$ ) was 6-fold faster than that of the WT TfRMAB-EPO fusion protein ( $19.4 \pm 6.9 \text{ mL}/\text{min}/\text{kg}$ ) (Table 1).

### Plasma pharmacokinetics after IP and SQ administration

The plasma concentrations-time curves following IP injections of a single 3 mg/kg dose of the TfRMAB-EPO and TfRMAB-N292G-EPO fusion proteins are shown in figure 4. The  $C_{\text{max}}$  of the WT TfRMAB-EPO fusion protein post IP administration was  $1.4 \pm 0.37 \mu\text{g}/\text{mL}$  ( $2.1 \pm 0.38 \text{ \%ID}/\text{mL}$ ) and that for the TfRMAB-N292G-EPO fusion protein was 37-fold lower at  $0.038 \pm 0.007 \mu\text{g}/\text{mL}$  ( $0.05 \pm 0.01 \text{ \%ID}/\text{mL}$ ) (Figures 4A–D and Table 1). The plasma concentrations-time curves following SQ injections of a single 3 mg/kg dose of the TfRMAB-EPO and TfRMAB-N292G-EPO fusion proteins are shown in figure 5. Similar to the decline in the  $C_{\text{max}}$  values post IP administration with the N292G mutation, the  $C_{\text{max}}$  values declined 114-fold from  $4.8 \pm 0.5 \mu\text{g}/\text{mL}$  ( $6.1 \pm 0.64 \text{ \%ID}/\text{mL}$ ) for the TfRMAB-EPO fusion protein to  $0.042 \pm 0.014 \mu\text{g}/\text{mL}$  ( $0.057 \pm 0.011 \text{ \%ID}/\text{mL}$ ) for the TfRMAB-N292G-EPO fusion protein (Figures 5A–D and Table 1). Consistent with these results, the plasma AUC over 24h was 14- to 81-fold higher for the WT TfRMAB-EPO fusion protein compared with the N292G mutant fusion protein following IP and SQ administration (Table 1).

The bioavailability of TfRMAB-EPO and TfRMAB-N292G-EPO following IP administration was 35% and 23%, respectively, and >50% and 24%, respectively, following SQ administration (Table 1). The bioavailability values reported here are an approximation due to the use of  $\text{AUC}(0-\infty)$  instead of  $\text{AUC}(0-24\text{h})$  for the IV route and the >50% SQ bioavailability of TfRMAB-EPO is due to the use of  $\text{AUC}(0-\infty)$  instead of  $\text{AUC}(0-24\text{h})$ . However, since the  $\text{AUC}(0-60)$  and  $\text{AUC}(0-\infty)$  values following IV administration are almost identical for the TfRMAB-N292G-EPO (Table 1),  $\text{AUC}(0-\infty)$  is used as an approximation of  $\text{AUC}(0-24)$  and is not expected to significantly impact the bioavailability estimates for TfRMAB-N292G-EPO.

### Reticulocyte count and cell proliferation

As shown in Figure 6A, a single 3 mg/kg dose of the TfRMAB-EPO fusion protein resulted in a >90% reduction of reticulocyte count following IP, SQ and IV administration compared with saline-treated control mice, and these counts were significantly lower than those in the mice treated with the N292G mutant TfRMAB fusion protein. Following IV administration, the N292G mutant TfRMAB fusion protein resulted in a 55% reduction in reticulocyte counts compared with saline-treated control mice, however, the reticulocyte counts in the cTfRMAB-N292G-EPO-treated mice were significantly higher than that in mice treated with the WT TfRMAB fusion protein. No significant suppression of reticulocytes was observed when the TfRMAB-N292G-EPO fusion protein was administered by the IP or SQ routes (Figure 6A).

Both the WT and N292G mutant TfRMAB-EPO fusion proteins resulted in a significant increase in cell proliferation (~55% increase with the TfRMAB-EPO, ~43% increase with the TfRMAB-N292G-EPO) compared to untreated or vehicle treated brain microvascular

endothelial cells in vitro. The increase in cell proliferation with these fusion proteins was comparable to that with rhuEPO (~40% increase with rhuEPO) (Figure 6B), and no significant differences were observed between the TfRMAB-EPO, TfRMAB-N292G-EPO and rhuEPO treated cells.

## Discussion

In the current study, we examined the effect of the N292G mutation on the PK of plasma clearance of a high-affinity TfRMAB-EPO fusion protein at doses ranging between 0.3–3 mg/kg in mice. Our results show a marked increase in the plasma clearance of the mutant TfRMAB-N292G-EPO compared with the WT TfRMAB-EPO fusion protein. The increase in plasma clearance was associated with a profound decline in the plasma  $C_{max}$  of the mutant TfRMAB-N292G-EPO following SQ (114-fold decline) and IP (37-fold decline) administration. A 10-fold increase in the IV dose from 0.3 mg/kg to 3 mg/kg resulted in a 7- to 11-fold decline in plasma clearance of both the WT and N292G mutant TfRMAB fusion proteins, which is consistent with non-linear PK of plasma clearance of the TfRMAB fusion protein with an increase in injection dose. Further, a single 3 mg/kg dose of the WT TfRMAB-EPO resulted in marked reticulocyte suppression, and the mutant TfRMAB-N292G-EPO reduced, but did not abolish, reticulocyte suppression.

The TfRMAB-EPO is a heterotetrameric fusion protein with an overall predicted molecular weight of 181,960 Da, with the EPO dimer comprising 20% of the molecular weight (36,000 Da) of the heterotetramer.<sup>21</sup> Each light chain (LC) is composed of 214 AA, without the 19 AA signal peptide, and the predicted molecular weight of the LC is 23,554 Da. The HC of the fusion protein is composed of 611 AA, without the 19 AA signal peptide, and has a predicted molecular weight of 67,358 Da. This is consistent with the migration of the fusion protein on both the reducing and non-reducing SDS-PAGE (Figure 1A) and as reported previously for the WT TfRMAB-EPO.<sup>21</sup>

The Fc glycan domain of an antibody strongly influences IgG binding to the Fc $\gamma$ R, but not to the FcRn.<sup>22–24</sup> The antibody Fc domain binds to the FcRn in an acidic environment, protecting the antibody from catabolism,<sup>25</sup> and antibody variants with reduced FcRn binding, but unaltered Fc $\gamma$ R interaction, show accelerated plasma clearance.<sup>23</sup> On the other hand, removal of the Fc N-linked glycosylation site at position N297 by substituting Asn with, for example, Gly (N297G mutation) reduces Fc-Fc $\gamma$ R interaction and antibody effector function, without altering Fc-FcRn interactions.<sup>18</sup> At IDs of 5 mg/kg or higher, aglycosylated antibody variants with the N297G mutation retain plasma PK properties comparable to the WT antibody in primates and rodents.<sup>17–18</sup> However, some studies show faster clearance of aglycosylated antibodies for reasons that are not well defined.<sup>26–27</sup> The effect of aglycosylation on the PK of antibody plasma clearance further depends on the antibody isotype. The plasma clearance of an IgG1 antibody variant with a N297Q mutation remains unaltered, however the plasma clearance of an IgG3 antibody variant is significantly increased compared with the WT antibody.<sup>28</sup>

There is limited data on the effect of the N297G mutation on the PK of plasma clearance of TfRMAB fusion proteins, with only one study reporting no change in the plasma



concentration and clearance following a single high ID (50 mg/kg) of a low-affinity TfRMAb fusion protein with the N297G mutation.<sup>16</sup> However, in the current study, the N292G mutation dramatically altered the PK of plasma clearance of the high-affinity TfRMAb fusion protein. For therapeutic IV doses between 0.3 mg/kg to 3 mg/kg, there was a 6- to 8-fold increase in the plasma clearance of the TfRMAb-N292G-EPO compared to the WT TfRMAb-EPO following IV administration (Table 1). This increase in plasma clearance was associated with a concomitant 10-fold decrease in the MRT of the TfRMAb-N292G-EPO at the 3 mg/kg IV dose. There was however, an increase in the MRT of the TfRMAb-N292G-EPO at the 0.3 mg/kg IV dose which is attributed to a 10-fold higher volume of distribution of the N292G mutant TfRMAb-EPO at this low dose.

The potential mechanisms underlying the enhanced clearance of the N292G mutant TfRMAb fusion protein include 1) changes in receptor-mediated clearance of the TfRMAb fusion protein, and 2) increased sensitivity of the aglycosylated IgG fusion protein to proteases.<sup>28-29</sup> The TfRMAb-EPO fusion protein in the current study is bi-specific and its plasma clearance can be mediated by peripheral TfR that binds to the TfRMAb domain of the fusion protein and the EPOR that binds to the EPO domain of the fusion protein. Any alteration in the binding affinity to these receptors can therefore significantly impact the plasma clearance of the TfRMAb-EPO fusion portion *in vivo*. In the current study, the N292G mutation, however, did not significantly alter the binding of the TfRMAb fusion protein to either of these receptors and both the WT and N292G mutant TfRMAb-EPO fusion protein retained high-affinity binding to the TfR and EPOR evident from the low Kd values (Figure 1B and 1C, respectively). Comparable receptor binding affinities result in similar biological activity of the WT and N292G mutant fusion proteins in the current study (Figure 6B). Both WT and N292G mutant fusion proteins significantly increased the proliferation of brain endothelial cells *in vitro*, a finding which is attributed to the effect of EPO on cell proliferation.<sup>30</sup> The above findings confirm that the two fusion proteins discussed herein retain comparable affinity and biological activity.

Non-linearity of the PK of plasma clearance of the TfRMAb fusion protein was observed in this study. A 10-fold increase in the IV injection dose, from 0.3 mg/kg to 3 mg/kg, resulted in a 7- to 11-fold decrease in the plasma clearance for both the mutant and WT TfRMAb-EPO (Table 1). This observation parallels a similar finding in the Rhesus monkey, where elevations in the IV infusion dose of TfRMAb (not fused to a biologic) resulted in a decrease in plasma clearance of the TfRMAb.<sup>31</sup> This suggests that the TfR involved in the clearance of the fusion protein is partially saturated *in vivo* over this dose range in the mouse. Doses of the TfRMAb fusion protein, higher than the ones used in the current study, may further saturate plasma clearance of the TfRMAb and mask the acceleration in plasma clearance observed with low-doses (0.3–3 mg/kg) used in the current study. Low-affinity TfRMAb under development require many-fold higher therapeutic doses (20–50 mg/kg), which can mask the increase in clearance observed in the current study,<sup>5, 16</sup> and this may explain the absence of any change in plasma clearance between the N297G mutant and WT low-affinity TfRMABs at high IDs.<sup>16</sup>

Apart from the TfR and EPOR involved in plasma clearance of the TfRMAb-EPO fusion protein, glycoproteins including IgG and EPO can undergo glycan receptor mediated

clearance *in vivo*, and the glycan content of the glycoprotein can significantly impact this clearance pathway.<sup>29, 32</sup> The glycosylation patterns of recombinant IgGs produced using CHO cells are similar to those found in naturally occurring serum IgGs compared to the murine melanoma cells that introduce glycan moieties, not naturally occurring, to the recombinant IgGs.<sup>29</sup> Further, glycosylation patterns of IgGs produced using the ExpiCHO system are similar to those produced using stable CHO cell lines.<sup>33</sup> The use of different expression systems, ExpiCHO for the N292G mutant fusion protein versus CHO for the WT fusion protein, is therefore not expected to introduce major differences in the glycosylation patterns between the WT and N292G mutant TfRMAB fusion proteins in the current study. In addition to glycosylation of the IgG domain of the WT fusion protein, the EPO domain of either the WT or mutant fusion protein is extensively glycosylated.<sup>34</sup> The usual post-translational modification and glycan content assays were not done because extensive glycosylation pattern of the EPO domain dwarfs the small differences in glycosylation of the IgG domain of the WT and mutant fusion proteins. In one assay, reducing SDS-PAGE can be used to show a slight reduction of the molecular weight of the glycosylated HC as compared to the aglycosylated HC, following an initial deglycosylation of the HC with N-glycanase. However, such molecular weight differences would be obscured and difficult to detect, since the percent change in the molecular weight of the HC of the TfRMAB-EPO fusion protein is much smaller than the percent change in the molecular weight of the HC of the TfRMAB alone, owing to the heavy N-linked glycosylation of the EPO domain, which is present in both fusion proteins. In another approach, the monosaccharide content of the fusion protein can be performed after acid hydrolysis. However, the EPO domain, which is present in both fusion proteins, is very heavily glycosylated with 3 N-linked sites and 1 O-linked site,<sup>34</sup> which would obscure the much smaller differences in glycosylation of the TfRMAB HC domain. The HC of the fusion protein contains 4 N-linked glycosylation sites, and 3 of these are present in the EPO domain. The effect of the glycan receptor mediated clearance on the plasma clearance of the N292G mutant cannot be ruled out.

Aglycosylated IgGs are increasingly sensitive to proteases and it is postulated that either the glycan structure of a non-mutant WT IgG shields the IgG from protease cleavage, or aglycosylation introduces conformational changes that renders the IgG more susceptible to cleavage.<sup>28</sup> Whether the N292G mutant TfRMAB fusion protein is more susceptible to protease cleavage is not known, as the EPOR ELISA used to measure plasma concentrations of the fusion proteins requires the presence of intact EPO as well as TfRMAB domains of the fusion protein (Methods).

It is interesting to note that the  $C_{\max}$  of the N292G mutant protein is reduced compared to the  $C_{\max}$  of the WT protein following IV administration (Table 1), and the difference in  $C_{\max}$  is a function of the ID. At the low ID of 0.3 mg/kg, the  $C_{\max}$  of the WT protein is 3.0-fold higher than the  $C_{\max}$  of the mutant protein, but at the 3 mg/kg dose, the  $C_{\max}$  of the WT protein is only 1.6-fold higher than the  $C_{\max}$  of the mutant protein (Table 1). This suggests a very high-affinity component of the clearance of the mutant protein, which becomes saturated as the ID increases from 0.3 mg/kg to 3 mg/kg as noted by the very steep inverse relationship between  $C_{\max}$  and plasma clearance of the N292G mutant fusion protein in the current study (Figure 3C). This may explain the initial rapid decline in the plasma

concentrations of the N292G mutant followed by a decline more comparable to the WT after IV administration (Figure 2 and 3).

For chronic neurodegenerative diseases, including AD, the SQ route is the preferred route of administration in humans, and in the current study we investigated the effect of the N292G mutation on the plasma PK of the TfRMAB fusion protein following SQ treatment, and for comparison, following IP administration. The plasma  $C_{max}$  values of the TfRMAB-N292G-EPO were profoundly reduced following SQ (114-fold lower) and IP (37-fold lower) administration (Table 1). This decline in plasma  $C_{max}$  is not attributed to low systemic bioavailability, but is most likely a direct consequence of accelerated plasma clearance of the TfRMAB-N292G-EPO, since the systemic bioavailability of the mutant TfRMAB fusion protein is comparable to that of other biopharmaceuticals including EPO.<sup>35</sup> The accelerated clearance of the N292G mutant TfRMAB-EPO thus results in excessively low plasma concentrations following IP and SQ administration compared with the WT TfRMAB-EPO fusion protein.

Our recent work shows the protective effect of chronic treatment with a 3 mg/kg IP dose of the WT TfRMAB-EPO in AD mice, and similar protective effects of other TfRMAB fusion proteins at comparable doses have been demonstrated in mice following SQ and IP administration.<sup>9–10, 36</sup> The brain concentration following a 3mg/kg SQ dose with a  $C_{max}$  of  $\sim 4 \mu\text{g/mL}$  of a TfRMAB-based fusion protein ranges between  $\sim 0.6 \mu\text{g/g}$  at 6h to  $0.68 \mu\text{g/g}$  at 24h.<sup>8</sup> Since the cTfRMAB-EPO is 20% EPO based on AA sequence,<sup>21</sup> the brain concentration of EPO is predicted to be around 140 ng/g ( $\sim 4 \text{ nM}$  EPO) between 6h and 24h following a single 3 mg/kg SQ dose administration of the WT TfRMAB-EPO. The plasma  $C_{max}$  post SQ administration of the WT TfRMAB-EPO is approximately  $4.8 \mu\text{g/mL}$  and that of the N292G mutant TfRMAB-EPO is  $\sim 100$ -fold lower. Such low plasma concentrations of the N292G mutant TfRMAB are predicted to result in low picomolar brain concentration of the EPO fusion protein. Given the accelerated plasma clearance and profoundly low plasma concentrations of the TfRMAB-N292G-EPO following SQ and IP administration, it is conceivable that much higher doses will be required to compensate for the accelerated clearance and low plasma concentrations of the N292G mutant TfRMAB, and to achieve brain concentrations comparable to the WT TfRMAB. Any therapeutic benefits of the N292G mutant TfRMAB-EPO may therefore be offset by the high injection doses needed thereof to produce a therapeutic effect comparable to that produced by the WT TfRMAB-EPO.

The Fc effector function of certain TfRMABs results in both acute clinical signs and reticulocyte suppression.<sup>4, 6</sup> In the present study no acute clinical signs (example: prostrate appearance, reddish urine, lethargy) were observed. However, significantly reduced reticulocytes were observed within 24h after a single 3 mg/kg IV dose (Figure 6), which is consistent with the expression of a high-affinity Tfr, which binds both transferrin and TfRMABs, on these immature red blood cells.<sup>37</sup> Prior studies utilizing TfRMAB fusion proteins with a human IgG1 Fc domain, showed a similar reduction in reticulocytes which was associated with acute clinical signs within 24h following a single IV injection of high doses (5–50 mg/kg).<sup>4, 16</sup> In the current study, the N292G mutation within the mouse IgG1 Fc region of the TfRMAB-EPO partially reversed, but did not abolish, reticulocyte suppression

after IV administration, which is consistent with previous findings showing partial reversal of reticulocyte suppression with an effectorless TfRMAb fusion protein dosed in mice lacking the Fc $\gamma$ R or WT mice.<sup>4</sup> This residual suppression of reticulocytes in the aforementioned study is attributed to the complement cascade.<sup>4</sup> Notably, reticulocyte suppression did not correlate with the plasma concentrations of the WT TfRMAb-EPO in the current study. For example, the  $C_{\max}$  of the WT fusion protein following IP administration is 15-fold lower than that following IV administration of the same dose (Table 1), but the reticulocyte levels remain very low after either IP or IV administration of the WT fusion protein (Figure 6). This is consistent with previous work in which a 10-fold dose reduction did not reverse reticulocyte suppression by a high-affinity TfRMAb fusion protein.<sup>4</sup> However, following IP and SQ administration of the TfRMAb-N292G-EPO, the reticulocyte counts returned back to normal (Figure 6), and this reversal of reticulocyte levels may be attributed to increased plasma clearance and profoundly low plasma  $C_{\max}$  values of the TfRMAb-N292G-EPO following IP and SQ administration.

In summary, the N292G mutant TfRMAb-EPO fusion protein mitigates the reticulocyte suppression associated with the WT TfRMAb-EPO fusion protein; however, the N292G mutation increases the clearance of the fusion protein resulting in profoundly low plasma  $C_{\max}$  values after SQ or IP administration. Thus, beneficial suppression of the effector function may be offset by the deleterious effect this mutation has on the plasma levels of the TfRMAb-EPO fusion protein, especially following SQ administration, which is the preferred route of administration in humans for chronic neurodegenerative diseases including AD. This is the first study, to the best of our knowledge, to characterize the impact of the N292G mutation on the PK of plasma clearance of a TfRMAb fusion protein following IV, SQ and IP administration. Given the recent interest in the development of effectorless TfRMAb fusion proteins, the effect of such mutations on the PK profile of TfRMAb fusion proteins needs further consideration.

## Acknowledgements

This work was supported in part by a grant from The National Institute of Health, NIA R21AG055949 (to RKS).

## Abbreviations

<b>OD</b>	Absorbance
<b>AD</b>	Alzheimer's disease
<b>AA</b>	Amino acids
<b>TfRMAb</b>	Transferrin receptor antibody
<b>AUC</b>	Area under the plasma concentration-time curve
<b>Asn</b>	Asparagine
<b>BBB</b>	Blood-brain barrier
<b>CHO</b>	Chinese hamster ovary

<b>K<sub>d</sub></b>	Dissociation constant
<b>ELISA</b>	Enzyme-linked immunosorbent assay
<b>EPO</b>	Erythropoietin
<b>EPOR</b>	Erythropoietin receptor
<b>FcγR</b>	Fc gamma receptor
<b>HC</b>	Heavy chain
<b>ID</b>	Injection dose
<b>IRR</b>	Injection related reactions
<b>IP</b>	Intraperitoneal
<b>IV</b>	Intravenous
<b>LC</b>	Light chain
<b>B<sub>max</sub></b>	Maximal binding
<b>C<sub>max</sub></b>	Maximum plasma concentration
<b>MRT</b>	Mean residence time
<b>MTHs</b>	Molecular Trojan horses
<b>FcRn</b>	Neonatal Fc receptor
<b>PK</b>	Pharmacokinetics
<b>RMT</b>	Receptor-mediated transcytosis
<b>SEC</b>	Size exclusion chromatography
<b>SQ</b>	Subcutaneous
<b>TfR</b>	Transferrin receptor
<b>TBS</b>	Tris-buffered saline
<b>TBST</b>	Tris-buffered saline containing 0.05% Tween-20
<b>TBSB</b>	Tris-buffered saline containing 1% bovine serum albumin
<b>V<sub>ss</sub></b>	Volume of distribution at steady-state
<b>WT</b>	Wild-type

## References

1. Qosa H; Volpe DA, The development of biological therapies for neurological diseases: moving on from previous failures. *Expert Opin Drug Discov* 2018, 13 (4), 283–293. [PubMed: 29394876]



2. Pardridge WM, The blood-brain barrier: bottleneck in brain drug development. *NeuroRx* 2005, 2 (1), 3–14. [PubMed: 15717053]
3. Pardridge WM, Blood-brain barrier drug delivery of IgG fusion proteins with a transferrin receptor monoclonal antibody. *Expert Opin Drug Deliv* 2015, 12 (2), 207–22. [PubMed: 25138991]
4. Couch JA; Yu YJ; Zhang Y; Tarrant JM; Fuji RN; Meilandt WJ; Solanoy H; Tong RK; Hoyte K; Luk W; Lu Y; Gadkar K; Prabhu S; Ordonia BA; Nguyen Q; Lin Y; Lin Z; Balazs M; Scearce-Levie K; Ernst JA; Dennis MS; Watts RJ, Addressing safety liabilities of TfR bispecific antibodies that cross the blood-brain barrier. *Sci Transl Med* 2013, 5 (183), 183ra57, 1–12.
5. Yu YJ; Zhang Y; Kenrick M; Hoyte K; Luk W; Lu Y; Atwal J; Elliott JM; Prabhu S; Watts RJ; Dennis MS, Boosting brain uptake of a therapeutic antibody by reducing its affinity for a transcytosis target. *Sci Transl Med* 2011, 3 (84), 84ra44.
6. Weber F; Bohrmann B; Niewoehner J; Fischer JAA; Rueger P; Tiefenthaler G; Moelleken J; Bujotzek A; Brady K; Singer T; Ebeling M; Iglesias A; Freskgard PO, Brain Shuttle Antibody for Alzheimer's Disease with Attenuated Peripheral Effector Function due to an Inverted Binding Mode. *Cell Rep* 2018, 22 (1), 149–162. [PubMed: 29298417]
7. Boado RJ; Zhang Y; Wang Y; Pardridge WM, Engineering and expression of a chimeric transferrin receptor monoclonal antibody for blood-brain barrier delivery in the mouse. *Biotechnol Bioeng* 2009, 102 (4), 1251–8. [PubMed: 18942151]
8. Sumbria RK; Zhou QH; Hui EK; Lu JZ; Boado RJ; Pardridge WM, Pharmacokinetics and brain uptake of an IgG-TNF decoy receptor fusion protein following intravenous, intraperitoneal, and subcutaneous administration in mice. *Mol Pharm* 2013, 10 (4), 1425–31. [PubMed: 23410508]
9. Chang R; Al Maghribi A; Vanderpoel V; Vasilevko V; Cribbs DH; Boado R; Pardridge WM; Sumbria RK, Brain Penetrating Bifunctional Erythropoietin-Transferrin Receptor Antibody Fusion Protein for Alzheimer's Disease. *Mol Pharm* 2018, 15 (11), 4963–4973. [PubMed: 30252487]
10. Sumbria RK; Hui EK; Lu JZ; Boado RJ; Pardridge WM, Disaggregation of amyloid plaque in brain of Alzheimer's disease transgenic mice with daily subcutaneous administration of a tetravalent bispecific antibody that targets the transferrin receptor and the Aβ amyloid peptide. *Mol Pharm* 2013, 10 (9), 3507–13. [PubMed: 23924247]
11. Sumbria RK; Boado RJ; Pardridge WM, Brain protection from stroke with intravenous TNFα decoy receptor-Trojan horse fusion protein. *J Cereb Blood Flow Metab* 2012, 32 (10), 1933–8. [PubMed: 22714051]
12. Zhou QH; Sumbria R; Hui EK; Lu JZ; Boado RJ; Pardridge WM, Neuroprotection with a brain-penetrating biologic tumor necrosis factor inhibitor. *J Pharmacol Exp Ther* 2011, 339 (2), 618–23. [PubMed: 21831964]
13. Yu YJ; Atwal JK; Zhang Y; Tong RK; Wildsmith KR; Tan C; Bien-Ly N; Hersom M; Maloney JA; Meilandt WJ; Bumbaca D; Gadkar K; Hoyte K; Luk W; Lu Y; Ernst JA; Scearce-Levie K; Couch JA; Dennis MS; Watts RJ, Therapeutic bispecific antibodies cross the blood-brain barrier in nonhuman primates. *Sci Transl Med* 2014, 6 (261), 261ra154.
14. Monnet C; Jorieux S; Urbain R; Fournier N; Bouayadi K; De Romeuf C; Behrens CK; Fontayne A; Mondon P, Selection of IgG Variants with Increased FcRn Binding Using Random and Directed Mutagenesis: Impact on Effector Functions. *Front Immunol* 2015, 6, 39. [PubMed: 25699055]
15. Saxena A; Wu D, Advances in Therapeutic Fc Engineering - Modulation of IgG-Associated Effector Functions and Serum Half-life. *Front Immunol* 2016, 7, 580. [PubMed: 28018347]
16. Lo M; Kim HS; Tong RK; Bainbridge TW; Vernes JM; Zhang Y; Lin YL; Chung S; Dennis MS; Zuchero YJ; Watts RJ; Couch JA; Meng YG; Atwal JK; Brezski RJ; Spiess C; Ernst JA, Effector-attenuating Substitutions That Maintain Antibody Stability and Reduce Toxicity in Mice. *J Biol Chem* 2017, 292 (9), 3900–3908. [PubMed: 28077575]
17. Leabman MK; Meng YG; Kelley RF; DeForge LE; Cowan KJ; Iyer S, Effects of altered FcγR binding on antibody pharmacokinetics in cynomolgus monkeys. *MAbs* 2013, 5 (6), 896–903. [PubMed: 24492343]
18. Jacobsen FW; Stevenson R; Li C; Salimi-Moosavi H; Liu L; Wen J; Luo Q; Daris K; Buck L; Miller S; Ho SY; Wang W; Chen Q; Walker K; Wypych J; Narhi L; Gunasekaran K, Engineering an IgG Scaffold Lacking Effector Function with Optimized Developability. *J Biol Chem* 2017, 292 (5), 1865–1875. [PubMed: 27994062]

19. Banks WA; Jumbe NL; Farrell CL; Niehoff ML; Heatherington AC, Passage of erythropoietic agents across the blood-brain barrier: a comparison of human and murine erythropoietin and the analog darbepoetin alfa. *Eur J Pharmacol* 2004, 505 (1–3), 93–101. [PubMed: 15556141]
20. Boado RJ; Hui EK; Lu JZ; Pardridge WM, Drug targeting of erythropoietin across the primate blood-brain barrier with an IgG molecular Trojan horse. *J Pharmacol Exp Ther* 2010, 333 (3), 961–9. [PubMed: 20233799]
21. Zhou QH; Boado RJ; Lu JZ; Hui EK; Pardridge WM, Re-engineering erythropoietin as an IgG fusion protein that penetrates the blood-brain barrier in the mouse. *Mol Pharm* 2010, 7 (6), 2148–55. [PubMed: 20860349]
22. Kim JK; Firan M; Radu CG; Kim CH; Ghetie V; Ward ES, Mapping the site on human IgG for binding of the MHC class I-related receptor, FcRn. *Eur J Immunol* 1999, 29 (9), 2819–25. [PubMed: 10508256]
23. Deng R; Meng YG; Hoyte K; Lutman J; Lu Y; Iyer S; DeForge LE; Theil FP; Fielder PJ; Prabhu S, Subcutaneous bioavailability of therapeutic antibodies as a function of FcRn binding affinity in mice. *MAbs* 2012, 4 (1), 101–9. [PubMed: 22327433]
24. Hinton PR; Johlfs MG; Xiong JM; Hanestad K; Ong KC; Bullock C; Keller S; Tang MT; Tso JY; Vasquez M; Tsurushita N, Engineered human IgG antibodies with longer serum half-lives in primates. *J Biol Chem* 2004, 279 (8), 6213–6. [PubMed: 14699147]
25. Kuo TT; Aveson VG, Neonatal Fc receptor and IgG-based therapeutics. *MAbs* 2011, 3 (5), 422–30. [PubMed: 22048693]
26. Xin Y; Jin D; Eppler S; Damico-Beyer LA; Joshi A; Davis JD; Kaur S; Nijem I; Bothos J; Peterson A; Patel P; Bai S, Population pharmacokinetic analysis from phase I and phase II studies of the humanized monovalent antibody, onartuzumab (MetMab), in patients with advanced solid tumors. *J Clin Pharmacol* 2013, 53 (11), 1103–11. [PubMed: 23922054]
27. Salgia R; Patel P; Bothos J; Yu W; Eppler S; Hegde P; Bai S; Kaur S; Nijem I; Catenacci DV; Peterson A; Ratain MJ; Polite B; Mehnert JM; Moss RA, Phase I dose-escalation study of onartuzumab as a single agent and in combination with bevacizumab in patients with advanced solid malignancies. *Clin Cancer Res* 2014, 20 (6), 1666–75. [PubMed: 24493831]
28. Tao MH; Morrison SL, Studies of aglycosylated chimeric mouse-human IgG. Role of carbohydrate in the structure and effector functions mediated by the human IgG constant region. *J Immunol* 1989, 143 (8), 2595–601. [PubMed: 2507634]
29. Liu L, Antibody glycosylation and its impact on the pharmacokinetics and pharmacodynamics of monoclonal antibodies and Fc-fusion proteins. *J Pharm Sci* 2015, 104 (6), 1866–1884. [PubMed: 25872915]
30. Anagnostou A; Lee ES; Kessimian N; Levinson R; Steiner M, Erythropoietin Has a Mitogenic and Positive Chemotactic Effect on Endothelial-Cells. *P Natl Acad Sci USA* 1990, 87 (15), 5978–5982.
31. Pardridge WM; Boado RJ; Patrick DJ; Ka-Wai Hui E; Lu JZ, Blood-Brain Barrier Transport, Plasma Pharmacokinetics, and Neuropathology Following Chronic Treatment of the Rhesus Monkey with a Brain Penetrating Humanized Monoclonal Antibody Against the Human Transferrin Receptor. *Mol Pharm* 2018, 15 (11), 5207–5216. [PubMed: 30226787]
32. Ashwell G; Harford J, Carbohydrate-specific receptors of the liver. *Annu Rev Biochem* 1982, 51, 531–54. [PubMed: 6287920]
33. Jain NK; Barkowski-Clark S; Altman R; Johnson K; Sun F; Zmuda J; Liu CY; Kita A; Schulz R; Neill A; Ballinger R; Patel R; Liu J; Mpanda A; Huta B; Chiou H; Voegtli W; Panavas T, A high density CHO-S transient transfection system: Comparison of ExpiCHO and Expi293. *Protein Expr Purif* 2017, 134, 38–46. [PubMed: 28342833]
34. Delorme E; Lorenzini T; Giffin J; Martin F; Jacobsen F; Boone T; Elliott S, Role of glycosylation on the secretion and biological activity of erythropoietin. *Biochemistry* 1992, 31 (41), 9871–6. [PubMed: 1390770]
35. Macdougall IC; Roberts DE; Neubert P; Dharmasena AD; Coles GA; Williams JD, Pharmacokinetics of recombinant human erythropoietin in patients on continuous ambulatory peritoneal dialysis. *Lancet* 1989, 1 (8635), 425–7. [PubMed: 2563798]

36. Chang R; Knox J; Chang J; Derbedrossian A; Vasilevko V; Cribbs D; Boado RJ; Pardridge WM; Sumbria RK, Blood-Brain Barrier Penetrating Biologic TNF-alpha Inhibitor for Alzheimer's Disease. *Mol Pharm* 2017, 14 (7), 2340–2349. [PubMed: 28514851]
37. Shumak KH; Rachkewich RA, Transferrin receptors on human reticulocytes: variation in site number in hematologic disorders. *Am J Hematol* 1984, 16 (1), 23–32. [PubMed: 6320639]

Author Manuscript

Author Manuscript

Author Manuscript

Author Manuscript

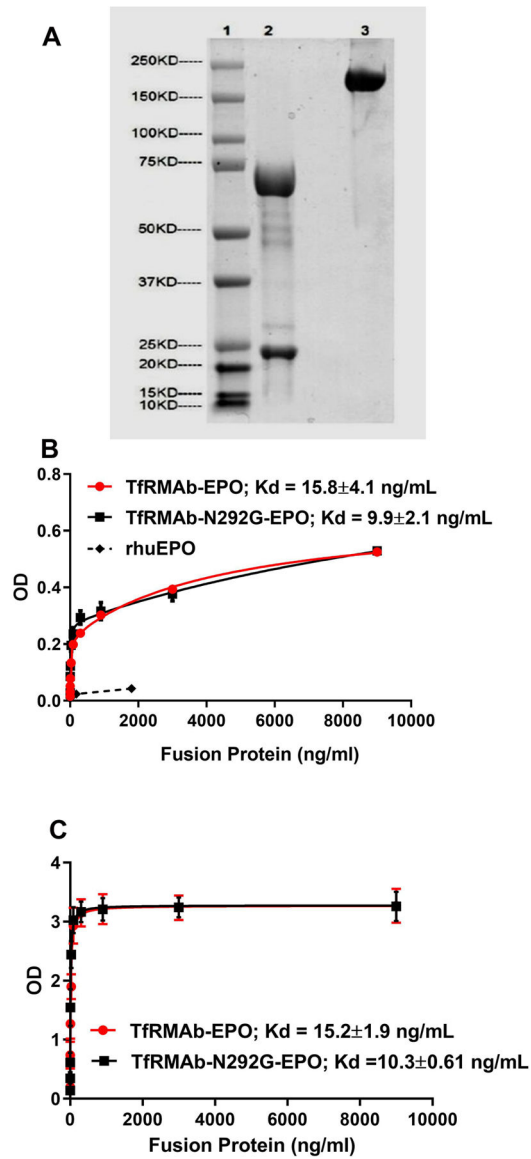


**Figure 1.** SDS-PAGE analysis of TfrMAb-N292G-EPO under reducing (lane 2) and non-reducing (lane 3) conditions (A). High-affinity binding of the WT and N292G mutant TfrMAb-EPO fusion proteins to TfR (B) and EPOR (C).

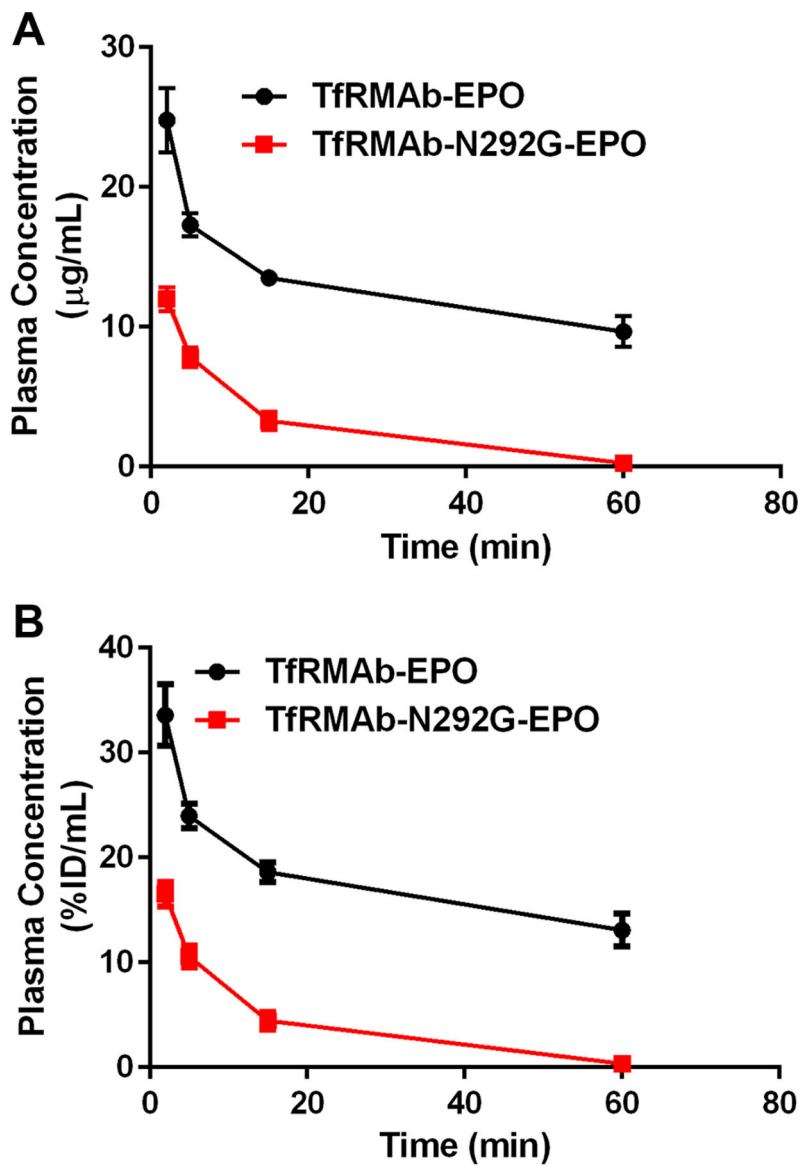


**Figure 2.** Plasma concentrations versus time curves following a single 3 mg/kg IV dose of TfRMAb-EPO (n=4) or TfRMAb-N292G-EPO (n=6) expressed as either (A)  $\mu\text{g/mL}$  or (B) %ID/mL. Data are shown as Mean  $\pm$  SEM.



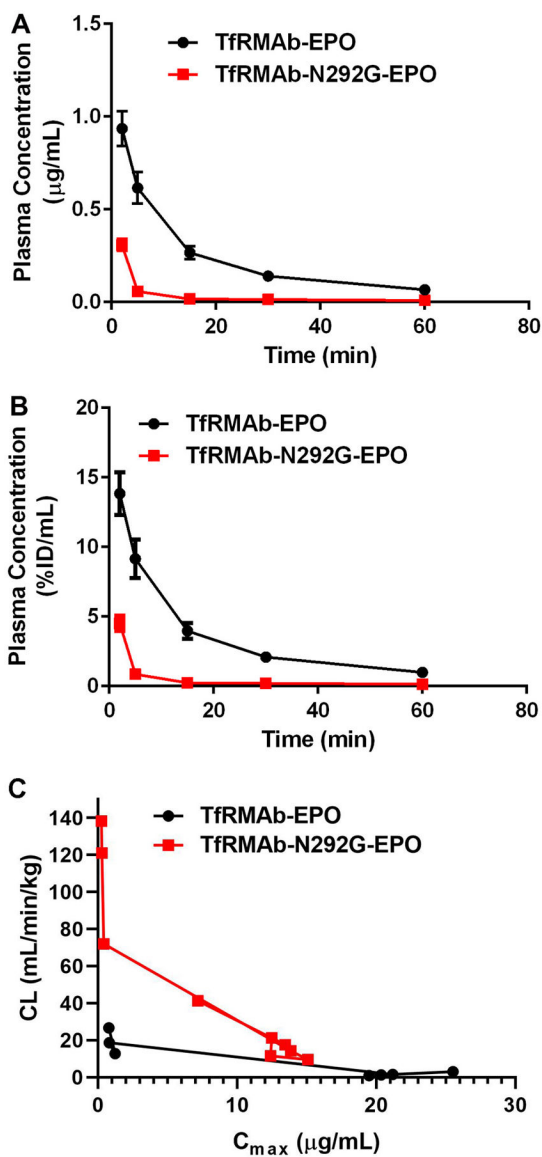


**Figure 3.** Plasma concentrations versus time curves following a single 0.3 mg/kg IV dose of TfRMAb-EPO (n=3) or TfRMAb-N292G-EPO (n=3) expressed as either (A)  $\mu\text{g/mL}$  or (B) %ID/mL. Inverse relationship between plasma clearance and  $C_{\text{max}}$  (C). Data are shown as Mean  $\pm$  SEM.

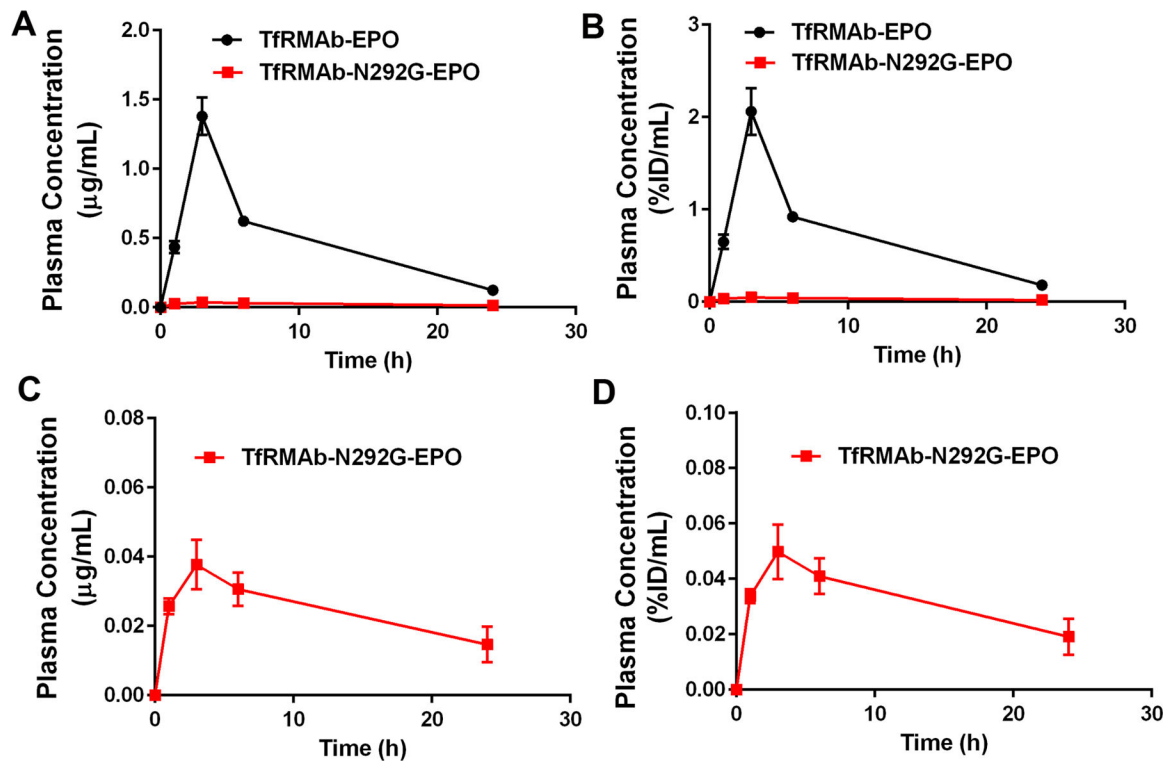


**Figure 4.** Plasma concentrations versus time curves following a single 3 mg/kg IP dose of TfRMAb-EPO (n=3) or TfRMAb-N292G-EPO (n=3) expressed as either (A, C)  $\mu\text{g/mL}$  or (B, D) %ID/mL. Data are shown as Mean  $\pm$  SEM.

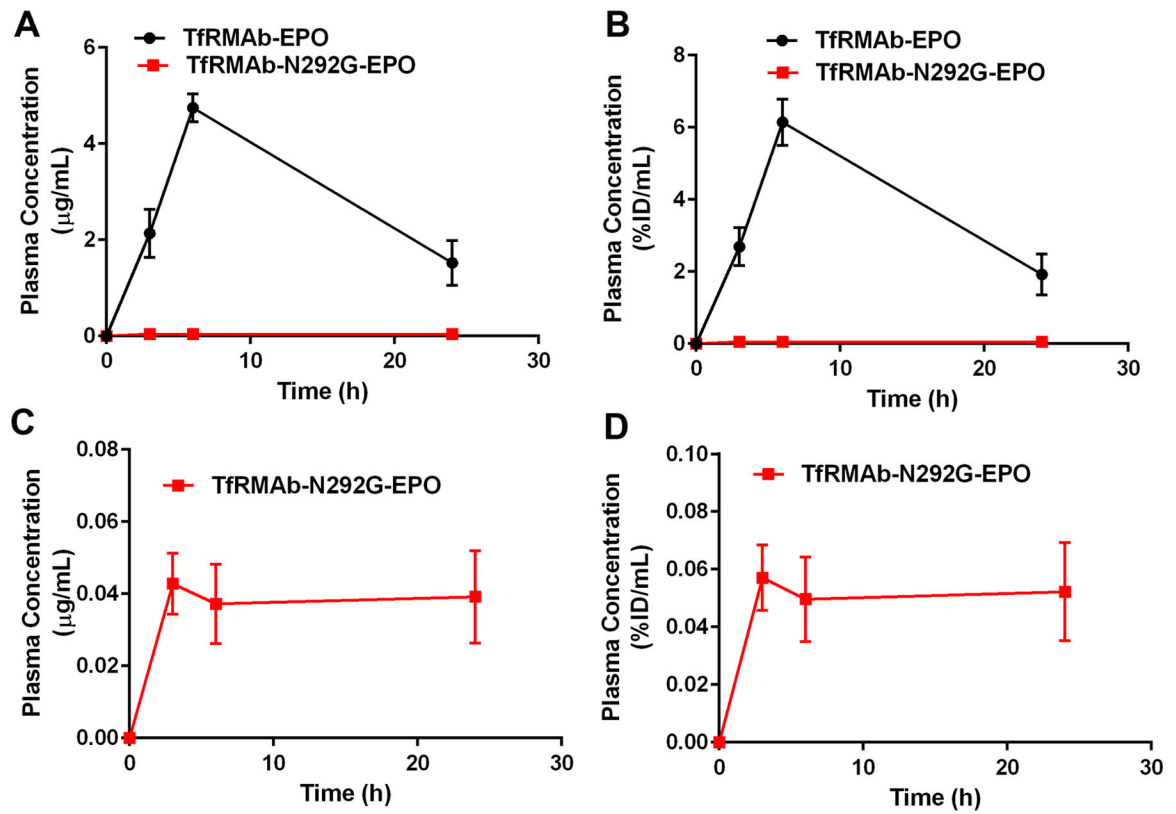


**Figure 5.**

Plasma concentrations versus time curves following a single 3 mg/kg SQ dose of TfRMAb-EPO (n=3) or TfRMAb-N292G-EPO (n=3) expressed as either (A, C)  $\mu\text{g/mL}$  or (B, D) %ID/mL. Data are shown as Mean  $\pm$  SEM.

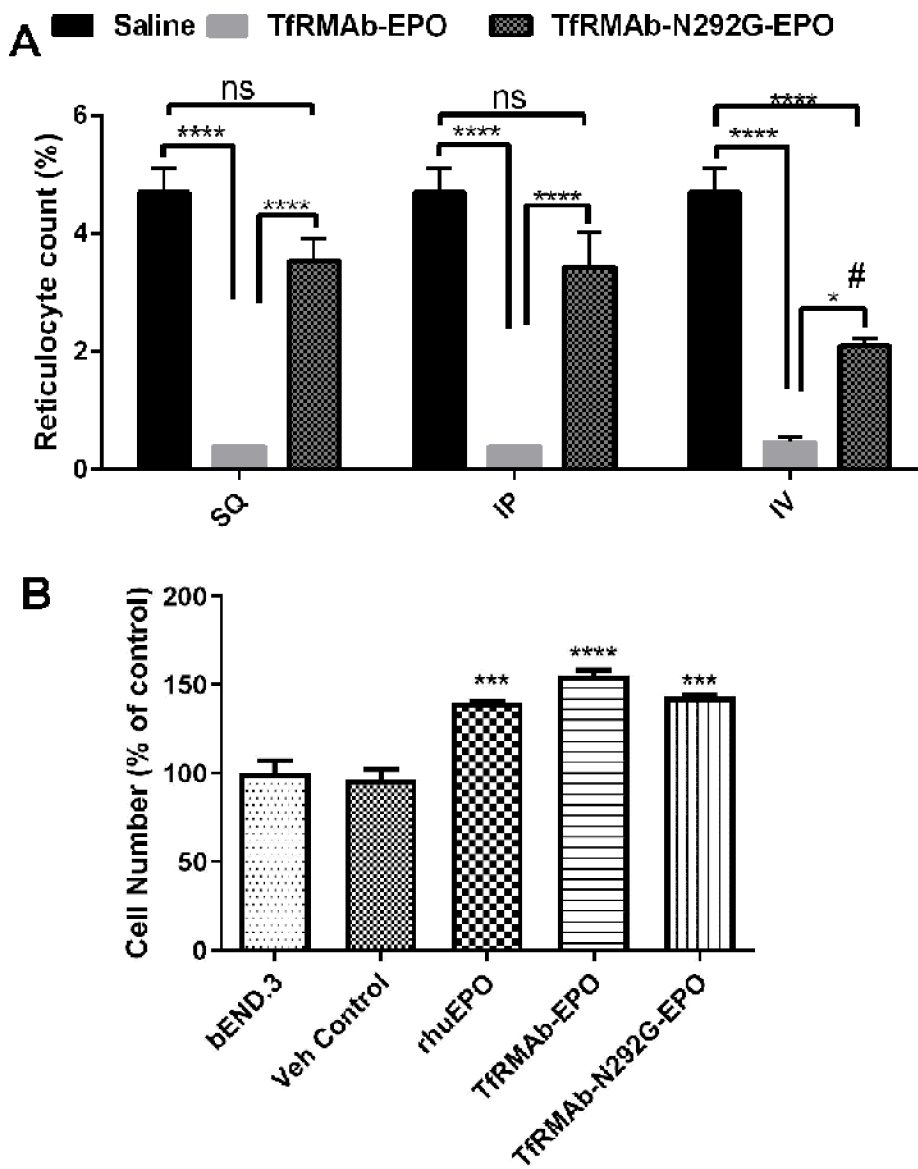


**Figure 6.** Reticulocyte counts (%) at 24h after a single 3 mg/kg SQ, IP or IV dose of saline (n=3), TfRMAB-EPO (n=3) or TfRMAB-N292G-EPO (n=3) (A). Cell number as an indicator of cell proliferation (% of bEND3 control) following 96h incubation with the indicated treatment (n=3) (B). Data are shown as Mean  $\pm$  SEM. \*P<0.05; \*\*\*\*P<0.0001 compared to the indicated group in A; #P<0.05 compared to the SQ injection of TfRMAB-N292G-EPO in A. \*\*\*\*P<0.0001, \*\*\*P<0.001 compared to bEND3 control in B. Statistical test: Two-way ANOVA with Bonferroni's post-hoc test for A and one-way ANOVA with Holm-Sidak's multiple comparisons test for B.

**Table 1.**

Non-compartmental pharmacokinetic parameters for TfRMAb-EPO and TfRMAb-N292G-EPO fusion proteins in the mouse following IV, IP, and SQ administration. Data is presented as mean  $\pm$  SEM.

Route of administration	PK Parameter	Parameter units	cTfRMAb-EPO	cTfRMAb-N292G-EPO
<b>IV 0.3 mg/kg</b>	C <sub>max</sub>	µg/mL	0.94 $\pm$ 0.3	0.31 $\pm$ 0.09
	MRT	min	24.5 $\pm$ 2.2	46.6 $\pm$ 15
	AUC(60 min)	µg•min/mL	14.9 $\pm$ 5.4	2.2 $\pm$ 0.6
	AUC(0–∞)	µg•min/mL	16.9 $\pm$ 6.1	2.9 $\pm$ 1.1
	V <sub>ss</sub>	mL/ kg	469 $\pm$ 142	4921 $\pm$ 1651
	Clearance	mL/min/kg	19.4 $\pm$ 6.9	110 $\pm$ 34
<b>IV 3 mg/kg</b>	C <sub>max</sub>	µg/mL	21.6 $\pm$ 2.7	13.5 $\pm$ 1.1
	MRT	min	116 $\pm$ 64	11.6 $\pm$ 2.9
	AUC(60 min)	µg•min/mL	800 $\pm$ 48	214 $\pm$ 67
	AUC(0–∞)	µg•min/mL	2045 $\pm$ 868	219 $\pm$ 70
	V <sub>ss</sub>	mL/ kg	159 $\pm$ 49	163 $\pm$ 23
	Clearance	mL/min/kg	1.8 $\pm$ 0.9	14.9 $\pm$ 4.7
<b>IP 3 mg/kg</b>	C <sub>max</sub>	µg/mL	1.4 $\pm$ 0.37	0.038 $\pm$ 0.007
	AUC (24 hrs)	µg•min/mL	705 $\pm$ 81	50 $\pm$ 30
	Clearance/F	mL/min/kg	4.3 $\pm$ 0.5	75 $\pm$ 39
	Bioavailability (F)	%	35	23
<b>SQ 3 mg/kg</b>	C <sub>max</sub>	µg/mL	4.8 $\pm$ 0.50	0.042 $\pm$ 0.014
	AUC (24 hrs)	µg•min/mL	4,198 $\pm$ 405	52 $\pm$ 27
	Clearance/F	mL/min/kg	0.72 $\pm$ 0.07	67 $\pm$ 28
	Bioavailability (F)	%	>50	24